AGU ADVANCING EARTH AND SPACE SCIENCE

JGR Space Physics

REVIEW ARTICLE
10.1029/2020JA028996

Special Section:
Solar and Heliospheric Plasma Structures: Waves, Turbulence, and Dissipation

Key Points:

- Alfvenicity is a crucial element, in addition to composition, for classifying the solar-wind in situ and identifying the source regions
- Similarities between Alfvenic slow and fast wind have been found at different radial distances during different phases of solar activity
- The solar sources of the Alfvenic slow wind streams have been recognized as regions of over-expanded magnetic flux tubes

Correspondence to:
R. D'Amicis,
raffaella.damicis@inaf.it

Citation:
D'Amicis, R., Perrone, D., Bruno, R., & Velli, M. (2021). On Alfvénic slow wind: A journey from the Earth back to the Sun. *Journal of Geophysical Research: Space Physics*, *126*, e2020JA028996. https://doi.org/10.1029/2020JA028996

Received 9 DEC 2020
Accepted 8 MAR 2021

On Alfvénic Slow Wind: A Journey From the Earth Back to the Sun

R. D'Amicis[1], D. Perrone[2], R. Bruno[1], and M. Velli[3]

[1]National Institute for Astrophysics, Institute for Space Astrophysics and Planetology, Rome, Italy, [2]ASI—Italian Space Agency, Rome, Italy, [3]University of California Los Angeles, Los Angeles, CA, USA

Abstract Comparative studies of fast and slow solar wind streams performed over the past decades have illustrated several differences between the plasma regimes for these different flows, examples including features such as temperatures, particle distribution function anisotropies, and the nature of the embedded turbulence, specifically the Alfvénicity of the fluctuations. Though this two-state classification of the solar wind primarily based on flow speed has been widely adopted, more in depth studies have found that slow solar wind should be further categorized, flow speed not being a sufficient descriptor of the plasma state. Within this framework, slow solar wind streams with a strong Alfvénic character have been identified and characterized, showing that in many ways they resemble fast solar wind. The similarities between fast and slow Alfvénic wind regimes have been explained in terms of a similar solar origin, with the latter corresponding to slow winds emanating from rapidly diverging low-latitude small coronal holes. The aim of this review is to describe the state of art of our understanding of Alfvénic slow solar wind streams. The results presented cover observations performed at different heliocentric distances spanning from Wind at L1 to Helios and Parker Solar Probe in the inner heliosphere, as well as a discussion of their source regions.

1. Introduction

"Asking for the average solar wind might appear as silly as asking for the taste of an average drink. What is the average between wine and beer? Obviously mere mixing—and averaging means mixing—does not lead to a meaningful result. Better taste and judge separately and then compare, if you wish." (Reiner Schwenn, Solar Wind 5, 1982) Following this basic idea, the quasi-stationary solar wind observed in the heliosphere has been traditionally categorized into two types based on particle bulk speed (Borovsky, 2012a; Stakhiv et al., 2015; Zurbuchen, 2007), namely fast ($V_{sw} > 600$ km/s) and slow ($V_{sw} < 500$ km/s) wind, also characterized by different features ranging from large to small scales. Indeed, slow wind has lower proton temperature and higher density, and in general much more variable properties, with respect to fast wind (Bruno et al., 1986; Lopez & Freeman, 1986; Schwenn, 2006). Moreover, the variability in the observed relative abundance of different charge-states of solar wind ions implies an anti-correlation of the freezing-in temperature with wind speed (Geiss et al., 1995; Kasper et al., 2012), and the thermodynamics of electrons, protons and heavy ions has also been observed to vary with speed (Hellinger et al., 2006; Kasper et al., 2008; Marsch, Rosenbauer, et al., 1982; Marsch, Schwenn, et al., 1982; Neugebauer et al., 1996; Matthaeus et al., 2006; Maruca et al., 2013, 2012; Matteini et al., 2013; Stansby et al., 2019), a strong correlation between speed and proton temperature being generally observed throughout (Burlaga & Ogilvie, 1970; Elliott et al., 2012; Grappin et al, 1990, 1991; Lopez & Freeman, 1986; Matthaeus et al., 2006; Perrone et al., 2019). Another difference between fast and slow wind related to plasma composition is the so called FIP effect: In the slow-speed wind, the abundance of elements having low first ionization potential (FIP ≤ 10 eV, i.e. low-FIP elements) is enhanced by a factor of 3–4 relative to photospheric, while in the fast speed their abundances are nearly photospheric (Geiss et al., 1995; Zurbuchen et al., 1999; von Steiger et al., 2000).

Slow solar wind in itself shows significantly variable properties: More recent characterizations, able to take into account the different features observed for fast and slow streams, discern the solar wind by its origin (see e.g., Camporeale et al., 2017; Stansby et al., 2018). Although it is generally accepted that fast solar wind originates from coronal holes (Cranmer, 2002; Geiss et al., 1995), the sources of slow solar wind are still under debate (Abbo et al., 2016, and references therein). In fact, if during solar minimum slow wind is usually observed close to the heliospheric current sheet (Bavassano et al., 1997; Smith et al., 1978), developing above (equatorial) coronal helmet streamer stalks, at solar maximum slow solar wind streams are interspersed with fast streams throughout the heliosphere (McComas et al., 2001), because the structure of the corona is very complex, with no large polar coronal holes and the presence of streamers and smaller coronal holes at all latitudes.

Although the standard classification of the solar wind on the average flow speed is widely accepted, it is not the only benchmark adopted to understand *in situ* observations. Marsch et al. (1981) first noticed in the Helios data acquired at 0.3 AU a slow wind interval that, apart from the speed, had much the same characteristics of the fast wind, such as a high degree of Alfvénicity.

Alfvénicity is a characteristic property of the observed turbulence fluctuations: Namely a high-degree of magnetic field (b)-velocity field (v) correlations, as in large amplitude Alfvén waves, with the correlation sign corresponding to waves propagating away from the Sun. The correlation is therefore positive in the presence of an ambient background field (B) of negative polarity connecting to the Sun, and negative in a background magnetic field of positive polarity. In addition to the $v-b$ correlation Alfvénic turbulence is characterized by weak compressibility (Zank & Matthaeus, 1992; Zank et al. 2017, and references thereis), in the sense that fluctuations in the magnitude of the total magnetic field are much smaller than the magnitude of the field fluctuations, and the relative density fluctuation magnitude is much smaller than the turbulent Mach number squared, $\delta n_p / n_p \ll (\delta v / V_{th})^2$, where n_p is the proton number density, δn and δv are the rms values of the density fluctuations and velocity fluctuations, $V_{th} = (2k_B T_p / m_p)^{1/2}$ is the thermal velocity of the plasma with k_B the Boltzmann constant, T_p the proton temperature, m_p the proton mass (Grappin et al., 1991).

Recently, analyzing solar maximum data, Alfvénic slow wind streams were observed for the first time at 1 AU (D'Amicis et al., 2011). Further examples of Alfvénic slow wind were extensively studied in their composition, thermodynamic, and turbulent characteristics (D'Amicis & Bruno, 2015; D'Amicis, Matteini, & Bruno, 2019), suggesting that fast and Alfvénic slow wind could have similar origin (D'Amicis & Bruno, 2015). Alfvénic slow wind at solar minimum has also been analyzed recently re-examining the Helios data collected in the inner heliosphere (Perrone, D'Amicis, et al., 2020; Stansby et al., 2018, 2020), the analysis supporting again a similar origin—coronal holes—for fast and slow Alfvénic wind streams. The recently launched Parker Solar Probe (PSP) also observed, over its first solar encounter at about 0.17 AU, long intervals of Alfvénic slow wind (Bale et al., 2019; Kasper et al., 2019). However, the most remarkable feature of the PSP observations was maybe the prevalence of large excursions in the radial magnetic field on all timescales, leading to local polarity reversals that had nothing to do with heliospheric current sheet crossings, but rather consisted in S-shaped magnetic field lines (Bale et al., 2019; Dudok de Wit et al., 2020). These so-called switchbacks are associated with intermittent radial velocity enhancements or jets, correlated to the radial magnetic field inversions in a way corresponding to Alfvénic turbulence (Horbury et al., 2020; Kasper et al., 2019).

This review provides a comprehensive discussion of the state of art on our understanding of Alfvénic slow solar wind streams, which represent a statistically important solar wind regime both in the inner heliosphere and at L1 throughout the solar cycle. The review is organized as follows: In Section 2 we present an overview of Alfvénic slow solar wind observations at different radial distances from the Sun. We decided to approach the description starting from observation in the near Earth environment, hence at L1, that corresponds also at the radial distance where the first in depth characterizations of this kind of wind have been performed; we then move to the observations in the inner heliosphere, at about 0.3 AU, collected by the Helios spacecraft more than 40 years ago; and finally, we present some of the very recent observations of Alfvénic slow solar wind collected by PSP over its first perihelia at about 0.17 AU from the Sun. In Section 3 we discuss the link between Alfvénic slow wind observed *in situ* and its source regions, to understand similarities shared with fast streams. Finally, in Section 4 we summarize the results and discuss open questions.

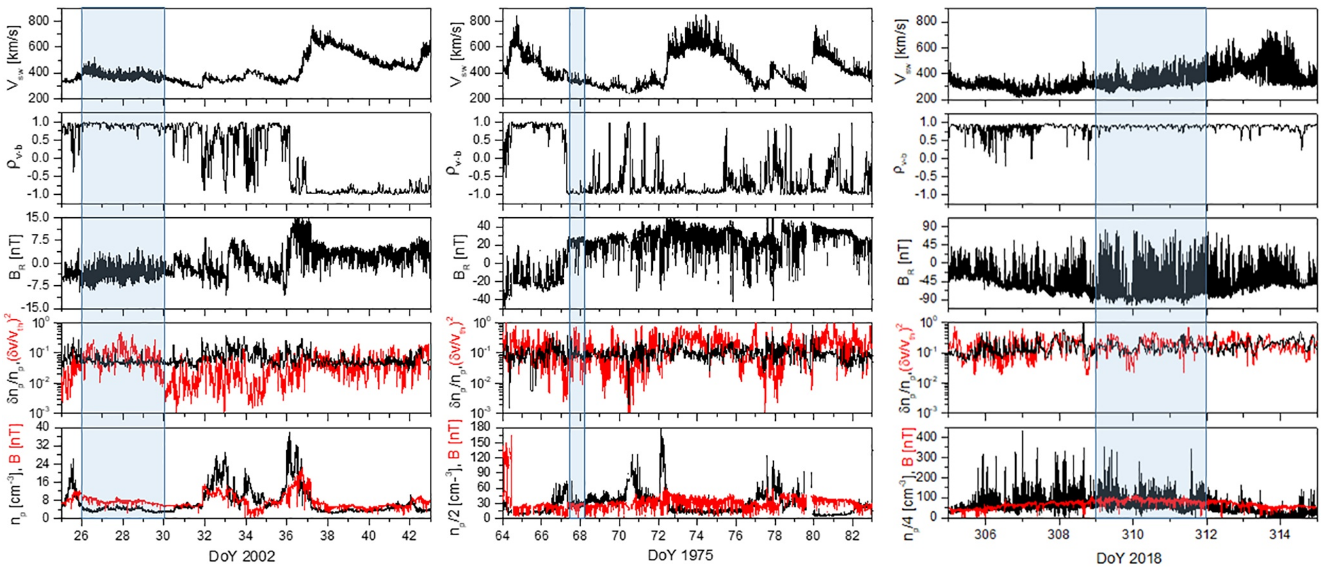

Figure 1. From left to right: Examples of Alfvénic slow wind intervals at 1 AU (Wind), 0.3 AU (Helios 1) and 0.17 AU (PSP), respectively, in color-filled bands. In each column, from top to bottom: Time series of solar wind bulk speed, V_{sw} (km/s); $v-b$ correlation coefficient, ρ_{v-b}, computed at 1 h scale; radial component of magnetic-filed vector, B_R (nT); $\delta n_p/n_p$ in black and $(\delta v\ /\ V_{th})^2$ in red for the condition of weak compressibility; and proton number density in black, n_p (cm^{-3}), and magnetic field magnitude in red, B (nT). PSP, Parker Solar Probe. The authors would like to thank Vincent Génot for useful discussions.

2. In Situ Observations

The first evidence of slow solar wind with a strong Alfvénic character was presented by Marsch et al. (1981) using Helios 2 data collected during the fifth perihelion passage, around 0.3 AU, in April 1978 during the ascending phase of solar activity. Indeed, those authors observed pronounced differential speeds between proton and alpha particles and large proton temperature anisotropies, similar to what is observed in fast wind streams but different from what had been seen in earlier observations of the slow wind at solar minimum. These features occurred simultaneously with the presence of highly Alfvénic fluctuations.

More recently, D'Amicis et al. (2011) performed a statistical study to characterize the state of solar wind turbulence at 1 AU during different phases of solar cycle 23. The study confirmed that solar minimum heliosphere is characterized by a bimodal solar wind structure (i.e., fast and slow streams) with fast wind being more Alfvénic than the slow wind. Moreover, during solar maximum, as expected, a predominance of slow wind was found. However, in contrast to previous studies (Belcher & Davis, 1971; Belcher & Solodyna, 1975), the slow solar wind streams were observed to belong to two populations characterized by very different, low and high, degrees of Alfvénicity.

The study of slow Alfvénic solar wind streams is now a very timely topic in space plasma physics, thanks to the very recent observations of PSP that observed, during its first perihelion encounter in November 2018, a long interval of highly Alfvénic, slow wind (Bale et al., 2019; Kasper et al., 2019). These measurements are allowing an in depth analysis of the Alfvénic slow wind in the inner heliosphere.

Figure 1 shows three reference samples of Alfvénic slow wind (color-filled bands) at different heliocentric distances, namely at 1 AU (left column), 0.3 AU (middle column) and 0.17 AU (right column), by using Wind, Helios 1 and PSP data, respectively. From top to bottom, for each time intervals, we show the solar wind bulk speed, V_{sw}; the $v-b$ correlation coefficient, ρ_{v-b}, computed at 1 h scale; the radial component of magnetic-filed vector, B_R; $\delta n_p/n_p$ and $(\delta v\ /\ V_{th})^2$; the proton number density, n_p, and magnetic field magnitude, B. The high ρ_{v-b} coefficient along with almost constant n_p and B and $\delta n_p\ /\ n_p \ll (\delta v\ /\ V_{th})^2$ (condition of weak compressibility) are clear indications of the presence of Alfvénic fluctuations, also highlighted by the presence of radial magnetic field inversions, that is switchbacks. Regarding the latter point, a supporting (but maybe not the dominant) generation mechanism for the Alfvénicity could be related to the presence of magnetic reconnection events. Indeed, the generation and emissions of Alfvén waves are expected in the interplanetary reconnection exhaust region (He et al., 2018).

2.1. Observation of Alfvénic Slow Wind at L1—Wind

A comprehensive characterization of the Alfvénic slow wind at 1 AU, based on a comparative study with the typical slow wind and fast wind, has recently been provided by D'Amicis, Matteini, and Bruno (2019). They found that, although Alfvénic and non-Alfvénic slow wind streams show similar bulk speeds, the former are characterized by the strong correlation between velocity and magnetic field fluctuations characteristic of outwardly propagating fluctuations with respect to the Sun. Moreover, in the Alfvénic slow wind, the magnetic field magnitude and number density are almost constant, suggesting a low compressibility (D'Amicis & Bruno, 2015), as expected for Alfvénic fluctuations. Conversely, the typical slow wind is more variable and high compressions are the main feature of these intervals. In particular, D'Amicis and Bruno (2015) showed that an anticorrelation exists between Alfvénicity and magnetic field compressibility, while no clear relationship was observed between Alfvénicity and number density compressibility. Furthermore, D'Amicis, Matteini, and Bruno (2019) found that, in both fast and slow Alfvénic winds, a well-defined correlation exists between the proton speed and the cosine of the angle between the magnetic field and the solar wind velocity direction. This correlation is a natural consequence of the Alfvénicity of the fluctuations, once one realizes that these fluctuations have quasi-spherical polarization (i.e., the magnetic field magnitude is essentially constant). Indeed, in such a situation, as the magnetic field rotates away from its background direction, the velocity field fluctuations must correspondingly deflect, to maintain the Alfvénic correlation. In all cases, outwardly propagating fluctuations produce radial velocity field enhancements: If the background field is outward, a rotation away will decrease its radial component, but the outward Alfvén wave has a negative $v-b$ correlation in this case, leading to a radial velocity enhancement. If the background field is inward, a rotation leads to a radial field increase, but in this case an outward propagating wave has a positive $v-b$ correlation, and the radial velocity field will again see an enhancement, as well discussed by Matteini et al. (2014, 2015). The extreme case is that of switchbacks in which the rotation of the field is greater than 180°. Note that Figure 1 actually displays this one sided enhancement of the radial velocity that appears as positive jetting in the Alfvénic solar wind periods.

Another interesting feature characterizing Alfvénic wind streams is the behavior of the Coulomb collisional age (A_C), a measure of the efficacy of Coulomb collisions in relaxing distribution functions during the solar wind transit from the Sun to the spacecraft (Kasper et al., 2008). D'Amicis, Matteini, and Bruno (2019) showed that Alfvénic winds are less collisional, irrespective of their speed, than the typical slow wind, with the fast wind showing the lowest A_C values. A low value of A_C is associated with a plasma that has experienced fewer Coulomb collisions and that might better preserve any signatures of wave-particle collisionless interactions occurring in the inner corona during wind acceleration, an important tool for the investigation of the solar wind source regions. Another crucial tool is the measurement of solar wind composition. In fact, the solar wind plasma composition is determined close to the Sun by plasma processes occurring in the upper chromosphere - transition region and within a few $R_\odot$, thus providing a connectivity tracer between solar sources and in situ measurements. D'Amicis, Matteini, and Bruno (2019) investigated the behavior of in situ composition signatures of the Alfvénic slow solar wind, suggesting a similar source for both fast and slow Alfvénic streams. This topic will be further discussed in Section 3.

Alfvénic intervals are also easily identified in the time series thanks to their enhanced velocity and magnetic field fluctuations with respect to periods of low Alfvénic correlation. The comparison between the power spectra of magnetic (D'Amicis, Matteini, & Bruno, 2019; D'Amicis et al., 2020) and velocity (D'Amicis et al., 2020) field fluctuations, for different solar wind regimes, shows that Alfvénic wind streams are characterized by higher power than that corresponding to the non-Alfvénic wind. This behavior is related to a larger amplitude of the fluctuations, typical of the presence of Alfvénic fluctuations. Moreover, fast and Alfvénic slow solar wind power spectra appear to be characterized, at large scales, by a $1/f$ scaling and a break in the spectrum around a typical scale that depends on distance and typically lies in between tens of minutes and a few hours, that has been related to the turbulent age of fluctuations at a given scale (D'Amicis, Matteini, & Bruno, 2019). The $1/f$ scaling has also been shown to be associated with the saturation of magnetic field fluctuations to amplitudes comparable to those of the average field in both fast (Matteini et al., 2018) and slow (Bruno et al., 2019; D'Amicis et al., 2020; Perrone, D'Amicis, et al., 2020) wind. However, for the non-Alfvénic slow wind, the $1/f$ scaling is recovered only if the interval is long enough to properly capture the low-frequency spectral properties and when perpendicular, directional, fluctuations are much larger than the compressive ones (Bruno et al., 2019). At shorter periods, below the break, a Kolmogorov-like power spectrum with index close to $-5/3$ is found for the magnetic field fluctuations, while velocity power spectra are systematically flatter with and index closer to the Iroshnikov-Kraichnan scaling of $-3/2$. On the contrary, typical slow wind is generally characterized by a Kolmogorov scaling over the whole frequency range from large to inertial scales, even if the $1/f$ scaling can be found for long enough intervals (Bruno et al., 2019) as discussed above. Indeed, while the absolute power spectra show that the three solar wind regimes observed are associated with different total turbulent energies for both magnetic and velocity fields (the largest amplitudes being found in the fast wind and the smallest in typical slow wind), the normalized power spectra, that is, normalized to the mean field in the considered interval, clearly show that the amplitude of the fluctuations observed in the Alfvénic fast and slow wind streams is similar and larger than that observed in typical slow wind (D'Amicis et al., 2020).

Around the ion characteristic scales, another break in the magnetic field power spectra is observed, which separates the inertial range from the kinetic range. The location of the ion-scale spectral break seems to not directly depend on the Alfvénic content of the fluctuations rather mostly on the ion plasma beta, β, defined as the ratio between ion kinetic pressure and magnetic pressure (Chen et al., 2014; Wang, C. Tu, et al., 2018; Wang, C. Y. Tu, et al., 2018; Woodham et al., 2018). Actually, the Alfvénic slow wind is characterized by a higher Alfvén speed, $V_A = B / (\mu_0 \rho)^{1/2}$ (where μ_0 is the magnetic permeability and ρ the ion mass density), with respect to the thermal speed $V_{\rm th}$, thus determining $\beta < 1$. In the intervals of fast wind, instead, V_A and $V_{\rm th}$ are comparable, so that β is on average around 1. Moreover, in general, V_A and V_{th} are lower in the Alfvénic slow than in the fast wind and, thus, the kinetic break is located at lower frequencies (D'Amicis, Matteini, & Bruno, 2019). These results suggest that the evolution of the turbulent cascade at kinetic scales does not depend only on the source properties, but also on the local plasma state and its variation during expansion. Furthermore, the slightly different values of the plasma beta determine the behavior of the different solar wind regimes in the ($\beta_\parallel$, $T_\perp/T_\parallel$) space, which results in similarities between fast and Alfvénic slow streams. Indeed, a well-defined anti-correlation between $\beta_\parallel$ and temperature anisotropy (D'Amicis, Matteini, & Bruno, 2019) similar to the one found by Marsch et al. (2004) is observed, with the Alfvénic slow wind characterized by lower β and larger anisotropy (at least for the maximum values). The reader is also directed to previous studies on the same topic at 1 AU performed over several years and merging different solar wind regimes (e.g. Bale et al., 2009; Kasper et al., 2002) or employing the standard classification of solar wind in fast and slow (e.g., Hellinger et al., 2006). However, further analysis is needed to better understand the dependence of the kinetic break on β.

2.2. Observations of Alfvénic Slow Streams Around 0.3 AU—Helios

Early observations of solar wind streams have shown the Alfvénic nature of fluctuations within the slow wind preceding the fast stream during the first Helios 2 perihelion passage occurred in 1976. In this particular interval, Bavassano et al. (1997) identified heliospheric current sheet crossing and were able to link the *in situ* observations to the interplanetary counterpart of the streamer stalk region, which is the narrow region in the middle of the streamer belt and which underlies the heliospheric current sheet. While the stalk has the highest density fluctuations and the lowest solar wind speeds, the density bumps are embedded in a density halo (which is still slow wind), a region with slightly higher density than the ambient which precedes the main portion of the fast stream. D'Amicis and Bruno (2015) found that Alfvénic correlations develop when passing through the interface between the stalk and the halo. Although being characterized by the same level of the v–b correlation coefficient, fluctuations within the halo have a smaller amplitude than those within the main portion of the fast stream.

Very recently, measurements from Helios solar probes have been used to detailed study, in the inner heliosphere, the Alfvénic slow solar wind. Stansby et al. (2020) performed a combination of proton, alpha particles, and electron measurements to investigate the kinetic properties of a single interval of Alfvénic slow wind observed by Helios 1 at 0.35 AU. This Alfvénic slow interval is characterized by high alpha particle abundances, similar to the one of the fast wind, whereas in the non-Alfvénic wind is significantly smaller. Moreover, for the Alfvénic slow wind they found a more pronounced alpha-proton differential streaming and large alpha-to-proton temperature ratios with respect to the non-Alfvénic slow wind. These features are also consistently observed in the fast wind. Furthermore, the analysis of the proton number density flux, normalized to the radial distance, shows that Alfvénic slow wind has a flux around twice that of the fast wind, and the non-Alfvénic wind has larger fluxes, around four times the fast wind flux. For what concern proton beams, the Alfvénic slow wind has a significantly higher beam fraction, in contrast to the non-Alfvénic wind which has a very low proton beam fraction. Finally, the electron (perpendicular) temperature in the Alfvénic slow interval ($\sim$2 10^5K) is twice that of the fast wind ($\sim$$10^5$K), but is a bit cooler with respect to the non-Alfvénic wind ($\sim$2.5 10^5K). The similarities observed between the fast and the Alfvénic slow wind suggest a common origin.

A complementary study has been performed by Perrone, D'Amicis, et al. (2020), who compared three different intervals of solar wind, namely fast, Alfvénic slow and non-Alfvénic slow, in terms of Alfvénic content and spectral properties, during a minimum phase of the solar activity and at 0.3 AU. Due to the Alfvénic nature of the fluctuations in both fast and Alfvénic slow wind, a well-defined correlation between the flow speed and the angle between magnetic field vector and radial direction has been found. This correlation stems from the $v-b$ correlation typical of Alfvénic fluctuations as well as their property of having an almost constant magnetic field magnitude. On the other hand, the speed in non-Alfvénic slow wind intervals do not show this type of correlation between magnetic field deflection and wind speed. Furthermore, comparing the spectral properties for the three regimes, the authors found a different turbulence behavior between Alfvénic and non-Alfvénic winds, due to the different nature of the fluctuations. Alfvénic winds have larger amplitude power spectra with respect to the non-Alfvénic slow wind. However, in contrast to the results at 1 AU and at the maximum of the solar cycle where the amplitude of the magnetic field fluctuations in the Alfvénic winds are almost the same (D'Amicis, Matteini, & Bruno, 2019), at the minimum of the solar activity and at 0.3 AU the fast wind shows fluctuations with larger amplitude with respect to the Alfvénic slow wind. The same differences are found for the velocity field. Finally, only for the Alfvénic intervals, a break between the inertial range and large scales is observed, on timescales where Alfvénic correlations are higher. At scales larger than the location of the break, a characteristic $1/f$ power law is observed, as expected for fluctuations that are scale-independent and saturated to the amplitude of the local magnetic field.

2.3. Observations of an Alfvénic Slow Wind Much Closer to the Sun—Parker Solar Probe

During its first perihelion passage in November 2018, located at a heliocentric distance of $\sim 35R_\odot$, PSP was embedded in slow wind except for brief periods, and for most of the encounter the slow wind was also found to be Alfvénic (Bale et al., 2019; Kasper et al., 2019; Parashar et al., 2020). One of the interesting results from these first PSP observations was the ubiquitous presence of large and intermittent polarity reversals of the radial component of the magnetic field, namely *switchbacks*, with oscillation amplitudes comparable to the magnitude of the magnetic field (Bale et al., 2019). The switchbacks consist of S-shaped magnetic structures (Chhiber et al., 2020; Dudok de Wit et al., 2020; McManus et al., 2020; Mozer et al., 2020), and, as discussed above, are also naturally associated with localized radial velocity enhancements (Horbury et al., 2020; Kasper et al., 2019). Switchbacks have also previously been observed, in the fast wind, by other missions at different heliocentric distances (Balogh et al., 1999; Behannon & Burlaga, 1981; Borovsky, 2016; Kahler et al., 1996; Landi et al., 2006; Tsurutani et al., 1994; Yamauchi et al., 2002). However, switchback structures at 1 AU may not be the same when one looks for the truly sunward propagating Alfvén waves instead of the pseudo-sunward propagation due to magnetic deflection (He et al., 2015).

The switchbacks observed by PSP have also been analyzed in terms of magnetic properties, suggesting the presence of three different groups of large-scale (larger than the typical ion scales) structures, namely full reversals, Alfvénic- and compressional-like structures (Krasnoselskikh et al., 2020). The authors described these structures as localized twisted magnetic tubes moving with respect to the surrounding plasma, where flowing currents have been recovered at their surface. Some electromagnetic wave activity has also been observed (Krasnoselskikh et al., 2020). Moreover, Perrone, Bruno, et al. (2020) have studied magnetic properties at ion scales in three selected periods characterized by different switchbacks activity. They found that this range of scales appears to be characterized by a high level of intermittency, with the presence of non-compressive coherent events, such as current sheets, vortex-like structures, and wave packets identified as ion cyclotron modes. The low magnetic compressibility found by Perrone, Bruno, et al. (2020) are in agreement with both results in the inner heliosphere (Bavassano, Dobrowolny, Fanfoni, et al., 1982) and at 1 AU (Perrone et al., 2017) in fast solar wind. The presence of small-scale coherent structures during PSP's first encounter has also been highlighted by employing the partial variance of increments (PVI) technique (Greco et al., 2008). Qudsi et al. (2020) found a temperature enhancements near PVI events, suggesting a mechanism of heating in the young solar wind related to intermittency developed by turbulence similar to the one observed at 1 AU (Osman et al., 2011, 2012; Perrone et al., 2014; Wu et al., 2013).

The turbulent character of the Alfvénic slow stream observed by PSP has also been studied in detail. Chen et al. (2020) observed an increased turbulence energy level by more than an order of magnitude and a lower magnetic compressibility compared to the plasma measured at 1 AU. Moreover, in the inertial range of the turbulent cascade, they found for the Alfvénic slow stream a typical spectral index of about $-3/2$ for both magnetic and velocity fields and a dominance of outward-propagating Alfvénic fluctuations with respect to the inward-propagating ones. Due to this Alfvénic property, a high fluid-range energy transfer rate is also recovered (Bandyopadhyay et al., 2020). Then, at the end of the inertial range a spectral break is observed. Duan et al. (2020) have shown that in the Alfvénic slow wind the break manifests a radial dependence similar to fast wind, with the spectral break occurring around the ion cyclotron resonance scales (Bruno & Trenchi, 2014; D'Amicis, Matteini, & Bruno, 2019). A similarity between fast and Alfvénic slow wind is also recovered in the relation between $\beta_\parallel$ and $T_\perp/T_\parallel$, suggesting that Alfvénic slow wind is characterized by more anisotropic distribution functions than non-Alfvénic slow wind, as is also seen in the fast solar wind (J. Huang, et al., 2020), and in agreement with observations at 1 AU (D'Amicis, Matteini, & Bruno, 2019).

3. Solar Sources

To identify the solar wind source regions one must establish a link between direct *in situ* measurements of the plasma by a spacecraft and a corresponding region of the Sun or solar corona using remote sensing observations. Since the solar magnetic field, through the Zeeman effect, can be measured at the photosphere (and lower chromosphere), where its distribution is strongly intermittent and characterized by different structures such as granulation, supergranulation and sunspots, the mapping of this field into the heliosphere is not smooth and continuous. The solar wind can easily advect neighboring field lines whose source regions may be widely separate in scales up to large fractions of a solar radius. Therefore, it is very difficult to locate precisely the area from which the solar wind emerges via, for instance, backward extrapolation onto the solar surface.

Moreover, although the solar wind originates very close to the solar surface, it is accelerated significantly at least in the first 5–10 $R_\odot$, so that projecting the field backwards toward the Sun ballistically, that is using the measured velocity to map back in-situ measurements close to the Sun contains an intrinsic error determined by the acceleration profile (see also Schwartz & Marsch, 1983). Empirical methods rely on the so-called source-surface method, that stops the backwards projection down at about 2.5 $R_\odot$, below which the field is reconstructed using the photospheric measured field and a potential extrapolation with purely radial boundary condition at the source-surface. A zero order estimate may then be obtained if at least the polarity of the extrapolated and ballistically mapped fields coincide at the source surface. Additional methods are clearly required to verify and improve the mapping to the Sun.

Additional important tracers are the elemental abundance and freezing-in temperatures that are known to be different for slow and fast solar winds and for the corresponding regions, coronal holes, active regions, quiet sun and helmet streamers, in the corona. Several studies have shown that *in situ* features are generally characterized by a sharp transition when passing from fast to slow streams, with particular reference to heavy ion charge state and elemental abundances (e.g. Zurbuchen et al., 1999, and references therein). These quantities are intimately related to the properties of the solar wind source region since they are essentially fixed in the inner corona (and well below 10 $R_\odot$). Geiss et al. (1995) and von Steiger et al. (1997, 2000) have pointed out that the charge state composition clearly distinguishes a coronal-hole-associated solar wind from a streamer-associated slow solar wind. Furthermore, Zurbuchen et al. (2000) demonstrated that clear variations within low-speed solar winds also separate different sources of low-speed solar winds.

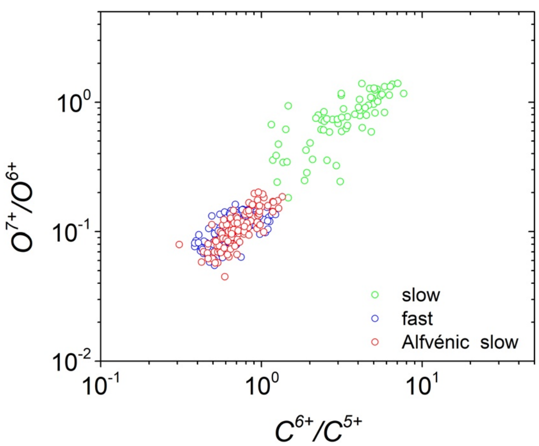

Figure 2. Scatter plot of oxygen ratio (O^{7+}/O^{6+}) and carbon ratio (C^{6+}/C^{5+}) for typical slow (green circles), fast (blue circles), and Alfvénic slow (red circles) solar winds. Adapted from D'Amicis, Matteini, and Bruno (2019). For the typical slow wind a slightly shorter time interval respect to the reference has been considered.

Particularly useful to distinguish between a coronal-hole-associated solar wind and a streamer-associated slow solar wind is the relation between O^{7+}/O^{6+} and C^{6+}/C^{5+} that freeze in rather close to the solar wind source region. These two quantities are clustered in well-defined regions of the $O^{7+}/O^{6+}–C^{6+}/C^{5+}$ space, depending on the solar wind regime observed (von Steiger, 2008), and are generally anticorrelated with flow speed. However, D'Amicis, Matteini, and Bruno (2019) showed that lower O^{7+}/O^{6+} and C^{6+}/C^{5+} characterize the Alfvénic time intervals (fast and slow) respect to the streamer-associated slow wind, occupying the same portion of the $O^{7+}/O^{6+}–C^{6+}/C^{5+}$ space and thus suggesting a similar solar origin of the two plasma flows. This is clearly shown in Figure 2, adapted from D'Amicis, Matteini, and Bruno (2019).

Therefore, these measurements provide important information, along with remote-sensing observations, about the regions of formation of the solar wind and, in particular, of the slow solar wind sources. This is a very hot topic since, although the source regions of fast wind streams have been unambiguously identified in polar coronal holes (Krieger et al., 1973; Zirker, 1977), the solar origin of slow wind is still debated. Indeed, Abbo et al. (2016) in their comprehensive review and references therein, identified the following solar sources and generation mechanisms for the slow solar wind: (i) high expansion factor of the magnetic topology adjacent to the helmet streamer, (ii) interchange reconnection between open field and closed loop in a helmet streamer, (iii) interchange reconnection between open field and closed loop in a pseudo-streamer, (iv) reconnection in complex magnetic structure with quasi-separatrix layers (S-Web model), (v) plasma blobs from closed loops at the cusp of a helmet streamer and (vi) open field structures in which turbulence/waves play a role in solar wind heating and acceleration.

The similar signatures found in both fast and Alfvénic slow wind (see e.g., D'Amicis & Bruno, 2015; D'Amicis, Matteini, & Bruno, 2019; D'Amicis et al., 2020; Perrone, D'Amicis, et al., 2020; Stansby et al., 2020; Telloni et al., 2020; Zhao et al., 2009) have suggested a similar origin for such wind streams even if the possibility that a slow wind can originate from coronal hole boundaries had been suggested previously. Indeed, Bravo and Stewart (1997) studied the variation of the plasma properties in a polar coronal holes from the center to the boundary and identified two different solar wind regimes: one at the central core related to fast wind streams and one at the boundary related to slower streams. They ascribed the lower temperature at the boundary to the strongly diverging and expanding field lines in the coronal hole boundaries and concluded that also medium- and low-latitude coronal holes would behave in a similar way taking into account also that the smaller size of the non-polar coronal holes might determine even much larger divergence. Neugebauer et al. (1998) confirmed previous results using several methods to map the solar wind observed by the Ulysses and Wind spacecraft to the solar surface. Their findings indicated that the fastest solar wind emanated from deep within the northern and southern polar coronal holes. Slower wind mapped to either the outer boundaries of the polar coronal holes, associated with the slow wind observed near the heliospheric current sheet, or to smaller coronal holes at low solar latitudes that typically replace polar coronal holes during sunspot maximum and were identified as the source regions of slow wind predominant during this phase of the solar cycle (Wang, 1994; Wang & Ko, 2019; Wang & Panasenco, 2019; Wang & Sheeley, 1990a). Moreover, UltraViolet Coronograph Spectrometer observations from the Solar and Heliospheric Observatory, highlighted the existence of two kinds of slow solar winds originating from different source regions, coronal streamers and either coronal hole boundaries or small coronal holes, respectively (Antonucci et al., 2005). Actually, small coronal holes ubiquitously observed during maximum of solar cycle 23 (Platten et al., 2014) were associated with different slow Alfvénic streams at 1 AU (D'Amicis, Matteini, & Bruno, 2019). It must be noted that both sources, that is, the low-latitude coronal holes and the boundaries of the polar coronal holes, are regions of anomalous (greater than average) areal expansion of magnetic flux tubes near the Sun, characterized by an inverse correlation of solar wind speed and flux-tube divergence rate (Levine et al., 1977; Wang & Sheeley, 1990b).

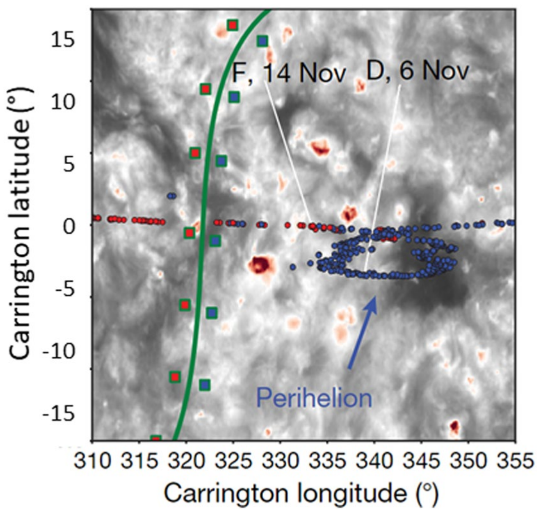

Figure 3. The extreme-ultraviolet synoptic map of 171 Å(Fe ix) emission during the first PSP perihelion passage, showing field lines mapping back to the Sun into a small equatorial coronal hole, identified as a lower density (darker) region and connected to the Alfvénic slow solar wind observed in situ by PSP. Indeed, the PSP trajectory at the source surface is marked by red and blue circles identifying positive and negative magnetic field polarities, respectively. The green line indicates the location of the adjacent model polarity-inversion line (PIL) associated with the heliospheric current sheet, from the 2 $R_{\odot}$ model, and blue and red squares refer to the polarity on either side of the model. Adapted from Bale et al. (2019).

On the other hand, the presence of Alfvénic slow streams is not a peculiar feature of the slow wind seen at solar maximum activity. Indeed, Alfvénic slow intervals have been also observed during sunspot minima in the inner heliosphere. Helios measurements of solar wind at 0.3 AU have allowed an in depth characterization of several Alfvénic slow streams, suggesting a most likely origin from equatorial extensions of polar coronal holes or from small, over-expanded, low-latitude coronal holes (D'Amicis & Bruno, 2015; Perrone, D'Amicis, et al., 2020; Stansby et al., 2020). Unfortunately, to our knowledge, there are no extreme ultraviolet images or magnetic field of the Sun available for the intervals where Helios observed Alfvénic slow streams. However, the recent and unique observations performed by PSP during its first perihelion passage at 0.17 AU have allowed connecting the Alfvénic slow wind origin to a coronal hole using the PFSS method (Panasenco et al., 2020; Badman et al., 2020). Global MHD models and magnetically mapping the s/c trajectory back to the solar surface, PSP was predicted to be connect a negative-polarity equatorial coronal hole, within which it remained for the entire encounter (Riley et al., 2019; Réville et al., 2020). With the PSP data becoming available, it has been possible to confirm that the *in situ* plasma associated with the small equatorial coronal hole is a highly Alfvénic slow wind stream, parts of which were also seen near Earth at L1 (Bale et al., 2019; Panasenco et al., 2020). Figure 3, adapted from Figure 1 in Bale et al. (2019), shows an extreme ultraviolet synoptic map whose magnetic field lines map back to the Sun into a low-latitude small coronal hole which was observed during PSP perihelion passage. Several analyses comparing PSP magnetic field measurements, during both the first and second encounters, to predictions obtained by potential field source surface (PFSS) modeling (Badman et al., 2020; Panasenco et al., 2020) or by MHD models (Réville et al., 2020) have been performed confirming that the Alfvénic slow wind observed by PSP originates from small equatorial coronal holes.

4. Discussion

In this review the properties of Alfvénic slow solar wind streams, observed throughout the heliosphere and in different periods of the solar cycle, have been summarized. The existence of such streams further supports the idea that the solar wind cannot be simply classified according to flow speed but that other properties, including composition and turbulence changes characteristics, should be taken into account (e.g. Camporeale et al., 2017; D'Amicis & Bruno, 2015; Ko et al., 2018; Perrone, D'Amicis, et al., 2020; Stakhiv et al., 2015; Stansby et al., 2018; von Steiger, 2008; Xu & Borovsky, 2015; Zhao et al., 2009). In this regard, studies of Alfvénic slow solar wind streams are particularly topical, as such streams, though rarely observed at solar minimum at heliocentric distances beyond 0.5 AU, appear to be very common especially during maximum of solar activity, and, has shown by the in situ observations collected by PSP in its first few orbits, also in the inner heliosphere inside the orbit of Mercury at solar minimum. Alfvénic slow wind shares several characteristics with the fast solar wind (see e. g. D'Amicis, Matteini, & Bruno, 2019; Stansby et al., 2018; Perrone, D'Amicis, et al., 2020, for details), especially in terms of Alfvénic content, even if its speed has similar values to those of the more standard slow solar wind seen at 1 AU (see Figure 1).

Alfvénic turbulence is of general interest in its own right, as it is thought to play a major role in coronal heating and solar wind acceleration, so that its generation, propagation and evolution in the heliosphere. For example, Alfvénic fluctuations might explain the correlation between the orientation of magnetic field non-compressive fluctuations and the perpendicular component of the proton temperature found in the fast wind and in the Alfvénic slow wind, via an ion cyclotron resonant mechanism (D'Amicis, De Marco, et al., 2019). This interpretation matches recent studies identifying signatures of ion-cyclotron waves within high speed plateau of typical corotating high velocity streams (Bruno & Telloni, 2015; Telloni &

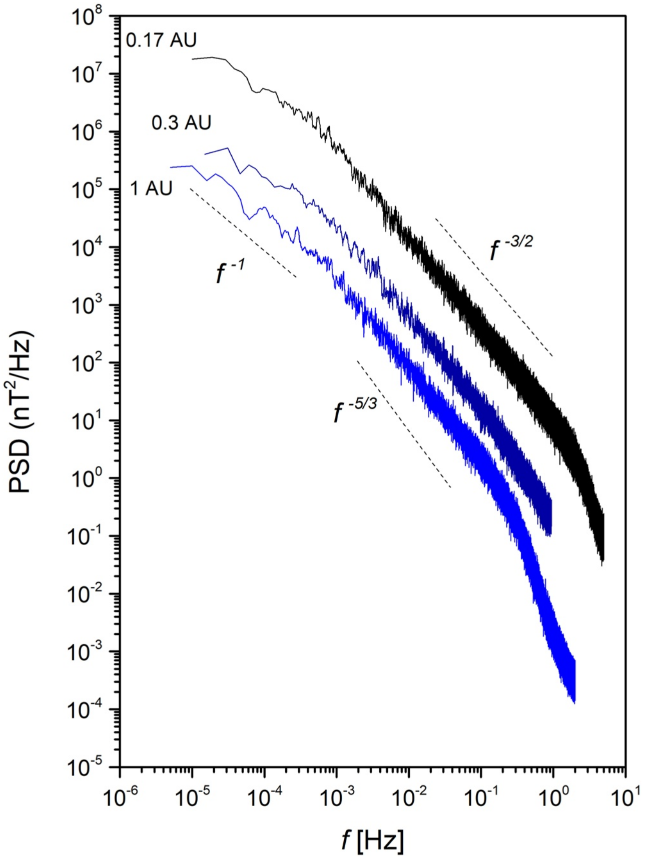

Figure 4. Power Spectral Density (PSD) of the trace of magnetic field fluctuations for Alfvénic slow wind intervals observed by Wind, Helios and PSP at 1 AU (blue), 0.3 AU (royal blue) and 0.17 AU (black), respectively. Kolmogorov ($f^{-5/3}$) and Kraichnan ($f^{-3/2}$) scalings in the inertial range, as well as the $1/f$ power law at injection scales, are shown for reference. A frequency cut in each PSD has been performed in order to remove noise effects.

Bruno, 2016) and in the Alfvénic slow wind (Telloni et al., 2020; S. Y. Huang, et al., 2020). The presence of ion-cyclotron waves might be related to fluid-scale Alfvénic fluctuations, characterizing intervals which would experience cyclotron resonance with protons (Bruno & Trenchi, 2014) causing an enhanced temperature anisotropy.

The similarities between the Alfvénic slow wind and the fast wind have an implication on the spectral features as well. As discussed above, Matteini et al. (2018) and Bruno et al. (2019) have shown that in the $1/f$ range of highly Alfvénic fast wind intervals, magnetic (and velocity field) fluctuations display a saturation at amplitudes of the background magnetic field. D'Amicis et al. (2020) have demonstrated that the same dynamics is recovered also for the Alfvénic slow wind at 1 AU, as long as the amplitude of velocity fluctuations is normalized to the effective phase velocity, v_ϕ, inferred by the local $v-b$ correlation. Therefore, the probability density functions of the magnetic and velocity fluctuations (normalized to the average magnetic field magnitude and v_ϕ, respectively) of the fast and Alfvénic slow wind coincide. Indeed, they are both centered around 1 and bounded between 0 and 2, as expected for fluctuations polarized on a sphere of constant radius B. This is in agreement with the presence of a $1/f$ range at large scales for both fields. The very close behavior in the properties of magnetic and velocity fluctuations is a direct consequence of the Alfvénic nature of the fluctuations. The same result has been shown at 0.3 AU (Perrone, D'Amicis, et al., 2020).

Figure 4 shows the Power Spectral Density (PSD) of the trace of magnetic field fluctuations for the Alfvénic slow wind intervals observed by Wind, Helios and PSP at 1 AU (blue), 0.3 AU (royal blue) and 0.17 AU (black), respectively. We use two days of data (except for Helios for which the Alfvénic slow interval is shorter) to also describe the low frequencies related to the injection range of the turbulence. Indeed, the presence of the $1/f$ regime described above is observed at all heliocentric distances. On the other hand, at intermediate scales (say the inertial range), the radial evolution suggests a transition from a Kraichnan-like scaling of the power density toward a Kolmogorov-like scaling when the heliocentric distance increases. This feature is in agreement with recent studies of the radial evolution of solar wind turbulence limited to PSP data (Chen et al., 2020; Duan et al., 2020). The same transition is recovered in the power spectrum of velocity fluctuations (not shown) but spread over a larger range of distances. Actually, although the PSD of velocity fluctuations is well described by a Kraichnan scaling at 1 AU (e.g. Podesta et al., 2006; Podesta et al., 2007; Salem et al., 2009; Borovsky, 2012b; D'Amicis et al., 2020), it has been shown by Roberts (2010) that it evolves toward $f^{-5/3}$ well past 1 AU, matching the theoretical prediction of the Kolmogorov theory.

Then, at the end of the inertial range, a spectral break, interpreted as a transition to kinetic turbulence, is observed. Figure 4 suggests that this break moves to lower frequencies as the solar wind travels in the inner heliosphere. The location of the kinetic break in magnetic field power spectra represents a highly debated topic in solar wind turbulent behavior. Indeed, this is a fundamental quantity for the identification of the dissipation mechanism responsible for the local heating of the solar wind plasma. Bruno and Trenchi (2014) first found the best agreement of the resonant wavenumber with the location of the kinetic break rather than with the ion inertial length or with the Larmor radius, in agreement with more recent papers (Duan et al., 2020; Perrone, Bruno, et al., 2020; Telloni et al., 2015; Wang, C. Tu, et al., 2018; Woodham et al., 2018). This applies to both Alfvénic and non-Alfvénic solar wind (D'Amicis, Matteini, & Bruno, 2019). It is also worth pointing out that inertial and kinetic scales are strongly linked. Indeed, higher power in the inertial range is related to steeper slopes in the in the first decade of frequency of the sub-ion range (Bruno et al., 2014), determining a well-defined separation between the fast and Alfvénic slow wind (higher power of the fluctuations and steeper spectra) and the non-Alfvénic slow wind (D'Amicis, Matteini, & Bruno, 2019).

The clear recognition of the existence and characterization of slow Alfvénic wind streams leads to a number of questions, both theoretical and observational, concerning their presence and evolution within the heliosphere throughout the solar cycle.

Important tracers of the solar sources are the elemental abundance and freezing-in temperatures, intimately related to the properties of the solar wind source region since they are essentially fixed in the inner corona. In situ elemental abundances of different charge-states (e.g., O^{7+}/O^{6+} and C^{6+}/C^{5+}) are generally characterized by a sharp transition when passing from fast to slow streams and can be used to discern between a coronal-hole solar wind from a streamer slow solar wind. However, Figure 2 clearly evidences a superposition between O^{7+}/O^{6+} and C^{6+}/C^{5+} values of the Alfvénic slow wind and the fast wind, at odds with previous observations (showing an anti-correlation between plasma composition and wind speed). This crucial result allows to identify the source regions of this Alfvénic slow wind as similar to those of the fast wind, that is coronal holes.

If both fast and slow wind may originate from coronal holes, then something must account for the difference in speed, and expansion factor appears to be the most promising. Although the identification of the source regions of the slow solar wind is still a matter of debate (e.g. Abbo et al., 2016), several authors agree that at least in the streams observed so far the region of origin appears to be an over-expanded equatorial small coronal hole (Antonucci et al., 2005; Bale et al., 2019; Neugebauer et al., 1998; Panasenco et al., 2020; Perrone, D'Amicis, et al., 2020; Wang, 1994; Wang & Ko, 2019; Wang & Panasenco, 2019; Wang & Sheeley, 1990a; Stansby et al., 2020) or, more in general, regions of anomalous (greater than average) areal expansion of magnetic flux tubes near the Sun. The larger expansion rate found for the Alfvénic slow wind with respect to the fast wind is also in agreement with the observed and well-established correlation between wind speed and proton temperature (e.g., Burlaga & Ogilvie, 1970; Elliott et al., 2012; Lopez & Freeman, 1986; Matthaeus et al., 2006; Perrone et al., 2019) which is valid at all radial distances also for the Alfvénic slow solar wind. In addition, electron temperature, in fast wind and Alfvénic slow wind, is lower than ion temperature even if in the latter the behavior is not always clear (D'Amicis, Matteini, & Bruno, 2019; Stansby et al., 2020).

Alfvénic turbulence has been shown to evolve in the heliosphere losing the characteristic dominance of outwardly propagating Alfvénic fluctuations. Early observations by Helios allowed to study the radial evolution of the same fast wind stream coming from the same source region, observed at three heliocentric distances (from 0.29 to 1 AU) after three successive solar rotations (Bavassano, Dobrowolny, Mariani, & Ness, 1982). Bruno et al. (2007) found that, as the wind expands, the Alfvénic content of these fluctuations decreases and the turbulent population, dominated at first by Alfvénic fluctuations in the fast wind at 0.29 AU, evolves toward a state dominated by smaller amplitude fluctuations and the appearance of another population, characterized by lower values of Alfvénicity and a clear imbalance in favor of magnetic energy. On the other hand, overall, the slow wind observed by Helios shows only a weak dependence on radial distance. However, the Alfvénic content of the fluctuations we find close to the Sun (at 0.3 AU for Helios and closer to the Sun with PSP) is rapidly lost when going to 1 AU. By contrast, observations by Wind at 1 AU during maximum of solar cycle (D'Amicis & Bruno, 2015) show a strong presence of Alfvénic fluctuations related to slow streams that resemble fast streams in many respects, including the speed profile (D'Amicis et al., 2020) except for the value of the speed itself. In such cases the question naturally arises of why Alfvénicity survives up to 1 AU in this case and not in others?

One possibility is that the different evolution depends on differences in the source region of this kind of slow wind. While we cannot comment on the solar source generating the slow wind observed by Helios, some insights may be provided by the recent PSP observations. Panasenco et al. (2020) performed a detailed study on the source of the highly Alfvénic wind observed at 0.17 AU and also on the Alfvénic wind observed at 1 AU that presumably evolved at that distance. They concluded that Alfvénicity decreases rapidly with distance from the streams close to the equator and the heliospheric current sheet, while it survives out to greater distances only in the fast wind from dominant polar coronal holes or in the slow wind from rapidly super-radially expanding small open "funnel" (Panasenco et al., 2019) regions.

Solar Orbiter, by combining both remote sensing observations and in situ measurements, will finally link the source regions on the Sun and the solar wind plasma properties. These upcoming data, along with PSP observations, will be of further support in characterizing the Alfvénic slow wind and in following the radial evolution of Alfvénicity in the inner heliosphere, helping to answer some of the above open questions.

Data Availability Statement

In the present research, all data come from previously published sources. Please refer to D'Amicis, Matteini, and Bruno (2019) for Wind data; Perrone, D'Amicis, et al. (2020) for Helios data; and Bale et al. (2019) for PSP data. Reprocessed particle data for Helios can be found in Stansby D., 2017, http://doi.org/10.5281/zenodo.1009506. WIND and PSP data are available on the NASA CDAWeb website: https://cdaweb.sci.gsfc.nasa.gov/.

Acknowledgments
M. Velli would like to thank the support from the FIELDS experiment on the Parker Solar Probe spacecraft, designed and developed under NASA contract NNN06AA01C as well as from the NASA HERMES DRIVE Science Center grant n. 80NSSC20K0604.

References

Abbo, L., Ofman, L., Antiochos, S. K., Hansteen, V. H., Harra, L., Ko, Y.-K. (2016). Slow solar wind: Observations and modeling. *Space Science Reviews*, *201*(1–4), 55–108. https://doi.org/10.1007/s11214-016-0264-1

Antonucci, E., Abbo, L., & Dodero, M. A. (2005). Slow wind and magnetic topology in the solar minimum corona in 1996–1997. *Astronomy & Astrophysics*, *435*(2), 699–711. https://doi.org/10.1051/0004-6361:20047126

Badman, S. T., Bale, S. D., Martínez Oliveros, J. C., Panasenco, O., Velli, M., Stansby, D., et al. (2020). Magnetic connectivity of the ecliptic plane within 0.5 au: Potential field source surface modeling of the first Parker Solar Probe encounter. *The Astrophysical Journal Supplement Series*, *246*(2), 23. https://doi.org/10.3847/1538-4365/ab4da7

Bale, S. D., Badman, S. T., Bonnell, J. W., Bowen, T. A., Burgess, D., Case, A. W., et al. (2019). Highly structured slow solar wind emerging from an equatorial coronal hole. *Nature*, *576*(7786), 237–242. https://doi.org/10.1038/s41586-019-1818-7

Bale, S. D., Kasper, J. C., Howes, G. G., Quataert, E., Salem, C., & Sundkvist, D. (2009). Magnetic fluctuation power near proton temperature anisotropy instability thresholds in the solar wind. *Physical Review Letters*, *103*(21), 211101. https://doi.org/10.1103/PhysRevLett.103.211101

Balogh, A., Forsyth, R. J., Lucek, E. A., Horbury, T. S., & Smith, E. J. (1999). Heliospheric magnetic field polarity inversions at high heliographic latitudes. *Geophysical Research Letters*, *26*(6), 631–634. https://doi.org/10.1029/1999GL900061

Bandyopadhyay, R., Goldstein, M. L., Maruca, B. A., Matthaeus, W. H., Parashar, T. N., Ruffolo, D., et al. (2020). Enhanced energy transfer rate in solar wind turbulence observed near the sun from Parker Solar Probe. *The Astrophysical Journal Supplement Series*, *246*(2), 48. https://doi.org/10.3847/1538-4365/ab5dae

Bavassano, B., Dobrowolny, M., Fanfoni, G., Mariani, F., & Ness, N. F. (1982). Statistical properties of MHD fluctuations associated with high-speed streams from Helios-2 observations. *Solar Physics*, *78*(2), 373–384. https://doi.org/10.1007/BF00151617

Bavassano, B., Dobrowolny, M., Mariani, F., & Ness, N. F. (1982). Radial evolution of power spectra of interplanetary Alfvénic turbulence. *Journal of Geophysical Research*, *87*(A5), 3617–3622. https://doi.org/10.1029/JA087iA05p03617

Bavassano, B., Woo, R., & Bruno, R. (1997). Heliospheric plasma sheet and coronal streamers. *Geophysical Research Letters*, *24*(13), 1655–1658. https://doi.org/10.1029/97GL01630

Behannon, K. W., & Burlaga, L. F. (1981). Alfven waves and Alfvenic fluctuations in the solar wind. *Solar Wind*, *4*, 374.

Belcher, J. W., Davis, L., & Leverett (1971). Large-amplitude Alfvén waves in the interplanetary medium, 2. *Journal of Geophysical Research*, *76*(16), 3534. https://doi.org/10.1029/JA076i016p03534

Belcher, J. W., & Solodyna, C. V. (1975). Alfvén waves and directional discontinuities in the interplanetary medium. *Journal of Geophysical Research*, *80*(1), 181. https://doi.org/10.1029/JA080i001p00181

Borovsky, J. E. (2012a). Looking for evidence of mixing in the solar wind from 0.31 to 0.98 AU. *Journal of Geophysical Research*, *117*(A6). https://doi.org/10.1029/2012JA017525

Borovsky, J. E. (2012b). The velocity and magnetic field fluctuations of the solar wind at 1 AU: Statistical analysis of Fourier spectra and correlations with plasma properties. *Journal of Geophysical Research*, *117*(A5). https://doi.org/10.1029/2011JA017499

Borovsky, J. E. (2016). The plasma structure of coronal hole solar wind: Origins and evolution. *Journal of Geophysical Research: Space Physics*, *121*(6), 5055–5087. https://doi.org/10.1002/2016JA022686

Bravo, S., & Stewart, G. A. (1997). Fast and slow wind from solar coronal holes. *The Astrophysical Journal Letters*, *489*(2), 992–999. https://doi.org/10.1086/304789

Bruno, R., D'Amicis, R., Bavassano, B., Carbone, V., & Sorriso-Valvo, L. (2007). Magnetically dominated structures as an important component of the solar wind turbulence. *Annales Geophysicae*, *25*(8), 1913–1927. https://doi.org/10.5194/angeo-25-1913-2007

Bruno, R., & Telloni, D. (2015). Spectral analysis of magnetic fluctuations at proton scales from fast to slow solar wind. *The Astrophysical Journal Letters*, *811*(2), L17. https://doi.org/10.1088/2041-8205/811/2/L17

Bruno, R., Telloni, D., Sorriso-Valvo, L., Marino, R., De Marco, R., & D'Amicis, R. (2019). The low-frequency break observed in the slow solar wind magnetic spectra. *Astronomy & Astrophysics*, *627*, A96. https://doi.org/10.1051/0004-6361/201935841

Bruno, R., & Trenchi, L. (2014). Radial dependence of the frequency break between fluid and kinetic scales in the solar wind fluctuations. *The Astrophysical Journal Letters*, *787*(2), L24. https://doi.org/10.1088/2041-8205/787/2/L24

Bruno, R., Trenchi, L., & Telloni, D. (2014). Spectral slope variation at proton scales from fast to slow solar wind. *The Astrophysical Journal Letters*, *793*(1), L15. https://doi.org/10.1088/2041-8205/793/1/L15

Bruno, R., Villante, U., Bavassano, B., Schwenn, R., & Mariani, F. (1986). In-situ observations of the latitudinal gradients of the solar wind parameters during 1976 and 1977. *Solar Physics*, *104*(2), 431–445. https://doi.org/10.1007/BF00159093

Burlaga, L. F., & Ogilvie, K. W. (1970). Heating of the solar wind. *The Astrophysical Journal Letters*, *159*, 659. https://doi.org/10.1086/150340

Camporeale, E., Carè, A., & Borovsky, J. E. (2017). Classification of solar wind with machine learning. *Journal of Geophysical Research: Space Physics*, *122*(11), 10910–10920. https://doi.org/10.1002/2017JA024383

Case, C. H. K., Leung, L., Boldyrev, S., Maruca, B. A., & Bale, S. D. (2014). Ion-scale spectral break of solar wind turbulence at high and low beta. *Geophysical Research Letters*, *41*(22), 8081–8088. https://doi.org/10.1002/2014GL062009

Chen, C. H. K., Bale, S. D., Bonnell, J. W., Borovikov, D., Bowen, T. A., Burgess, D., et al. (2020). The evolution and role of solar wind turbulence in the inner heliosphere. *The Astrophysical Journal Supplement Series*, *246*(2), 53. https://doi.org/10.3847/1538-4365/ab60a3

Chhiber, R., Goldstein, M. L., Maruca, B. A., Chasapis, A., Matthaeus, W. H., Ruffolo, D., et al. (2020). Clustering of intermittent magnetic and flow structures near Parker Solar Probe's first perihelion—A partial-variance-of-increments analysis. *The Astrophysical Journal Supplement Series*, *246*(2), 31. https://doi.org/10.3847/1538-4365/ab53d2

Cranmer, S. R. (2002). Coronal holes and the high-speed solar wind. *Space Science Reviews*, *101*(3), 229–294. https://doi.org/10.1023/a:1020840004535

D'Amicis, R., & Bruno, R. (2015). On the origin of highly Alfvénic slow solar wind. *The Astrophysical Journal*, *805*(1), 84. https://doi.org/10.1088/0004-637X/805/1/84

D'Amicis, R., Bruno, R., & Bavassano, B. (2011). Response of the geomagnetic activity to solar wind turbulence during solar cycle 23. *Journal of Atmospheric and Solar-Terrestrial Physics*, *73*(5–6), 653–657. https://doi.org/10.1016/j.jastp.2011.01.012

D'Amicis, R., De Marco, R., Bruno, R., & Perrone, D. (2019). Investigating the nature of the link between magnetic field orientation and proton temperature in the solar wind. *Astronomy & Astrophysics*, *632*, A92. https://doi.org/10.1051/0004-6361/201936728

D'Amicis, R., Matteini, L., & Bruno, R. (2019). On the slow solar wind with high Alfvénicity: From composition and microphysics to spectral properties. *Monthly Notices of the Royal Astronomical Society*, *483*(4), 4665–4677. https://doi.org/10.1093/mnras/sty3329

D'Amicis, R., Matteini, L., Bruno, R., & Velli, M. (2020). Large amplitude fluctuations in the Alfvénic solar wind. *Solar Physics*, *295*(3), 46. https://doi.org/10.1007/s11207-020-01606-2

Duan, D., Bowen, T. A., Chen, C. H. K., Mallet, A., He, J., Bale, S. D., et al. (2020). The radial dependence of proton-scale magnetic spectral break in slow solar wind during PSP encounter 2. *The Astrophysical Journal Supplement Series*, *246*(2), 55. https://doi.org/10.3847/1538-4365/ab672d

Dudok de Wit, T., Krasnoselskikh, V. V., Bale, S. D., Bonnell, J. W., Bowen, T. A., Chen, C. H. K., et al. (2020). Switchbacks in the near-sun magnetic field: Long memory and impact on the turbulence cascade. *The Astrophysical Journal Supplement Series*, *246*(2), 39. https://doi.org/10.3847/1538-4365/ab5853

Elliott, H. A., Henney, C. J., McComas, D. J., Smith, C. W., & Vasquez, B. J. (2012). Temporal and radial variation of the solar wind temperature-speed relationship. *Journal of Geophysical Research*, *117*(A9), A09102. https://doi.org/10.1029/2011JA017125

Geiss, J., Gloeckler, G., & von Steiger, R. (1995). Origin of the solar wind from composition data. *Space Science Reviews*, *72*(1–2), 49–60. https://doi.org/10.1007/BF0076875310.1007/978-94-011-0167-7_8

Grappin, R., Mangeney, A., & Marsch, E. (1990). On the origin of solar wind MHD turbulence: Helios data revisited. *Journal of Geophysical Research*, *95*(A6), 8197–8209. https://doi.org/10.1029/ja095ia06p08197

Grappin, R., Velli, M., & Mangeney, A. (1991). "Alfvénic" versus "standard" turbulence in the solar wind. *Annales Geophysicae*, *9*, 416–426.

Greco, A., Chuychai, P., Matthaeus, W. H., Servidio, S., & Dmitruk, P. (2008). Intermittent MHD structures and classical discontinuities. *Geophysical Research Letters*, *35*(19), L19111. https://doi.org/10.1029/2008GL035454

He, J., Pei, Z., Wang, L., Tu, C., Marsch, E., Zhang, L., & Salem, C. (2015). Sunward propagating Alfvén waves in association with sunward drifting proton beams in the solar wind. *The Astrophysical Journal Letters*, *805*(2), 176. https://doi.org/10.1088/0004-637X/805/2/176

He, J., Zhu, X., Chen, Y., Salem, C., Stevens, M., Li, H., et al. (2018). Plasma heating and Alfvénic turbulence enhancement during two steps of energy conversion in magnetic reconnection exhaust region of solar wind. *The Astrophysical Journal*, *856*(2), 148. https://doi.org/10.3847/1538-4357/aab3cd

Hellinger, P., Trávníček, P., Kasper, J. C., & Lazarus, A. J. (2006). Solar wind proton temperature anisotropy: Linear theory and WIND/SWE observations. *Geophysical Research Letters*, *33*(9), L09101. https://doi.org/10.1029/2006GL025925

Horbury, T. S., Woolley, T., Laker, R., Matteini, L., Eastwood, J., Bale, S. D., et al. (2020). Sharp Alfvénic impulses in the near-sun solar wind. *The Astrophysical Journal Supplement Series*, *246*(2), 45. https://doi.org/10.3847/1538-4365/ab5b15

Huang, J., Kasper, J. C., Vech, D., Klein, K. G., Stevens, M., Martinović, M. M., et al. (2020). Proton temperature anisotropy variations in inner heliosphere estimated with the first Parker Solar Probe observations. *The Astrophysical Journal Supplement Series*, *246*(2), 70. https://doi.org/10.3847/1538-4365/ab74e0

Huang, S. Y., Zhang, J., Sahraoui, F., He, J. S., Yuan, Z. G., Andrés, N., et al. (2020). Kinetic scale slow solar wind turbulence in the inner heliosphere: Coexistence of kinetic Alfvén waves and Alfvén ion cyclotron waves. *The Astrophysical Journal Letters*, *897*(1), L3. https://doi.org/10.3847/2041-8213/ab9abb

Kahler, S. W., Crocker, N. U., & Gosling, J. T. (1996). The topology of intrasector reversals of the interplanetary magnetic field. *Journal of Geophysical Research*, *101*(A11), 24373–24382. https://doi.org/10.1029/96JA02232

Kasper, J. C., Bale, S. D., Belcher, J. W., Berthomier, M., Case, A. W., Chandran, B. D. G., et al. (2019). Alfvénic velocity spikes and rotational flows in the near-sun solar wind. *Nature*, *576*(7786), 228–231. https://doi.org/10.1038/s41586-019-1813-z

Kasper, J. C., Lazarus, A. J., & Gary, S. P. (2002). Wind/SWE observations of firehose constraint on solar wind proton temperature anisotropy. *Geophysical Research Letters*, *29*(17), 20. https://doi.org/10.1029/2002GL015128

Kasper, J. C., Lazarus, A. J., & Gary, S. P. (2008). Hot solar-wind helium: Direct evidence for local heating by Alfvén-cyclotron dissipation. *Physical Review Letters*, *101*(26), 261103. https://doi.org/10.1103/PhysRevLett.101.261103

Kasper, J. C., Stevens, M. L., Korreck, K. E., Maruca, B. A., Kiefer, K. K., Schwadron, N. A., & Lepri, S. T. (2012). Evolution of the relationships between helium abundance, minor ion charge state, and solar wind speed over the solar cycle. *The Astrophysical Journal Letters*, *745*(2), 162. https://doi.org/10.1088/0004-637X/745/2/162

Ko, Y.-K., Roberts, D. A., & Lepri, S. T. (2018). Boundary of the slow solar wind. *The Astrophysical Journal Letters*, *864*(2), 139. https://doi.org/10.3847/1538-4357/aad69e

Krasnoselskikh, V., Larosa, A., Agapitov, O., de Wit, T. D., Moncuquet, M., Mozer, F. S., et al. (2020). Localized magnetic-field structures and their boundaries in the near-sun solar wind from Parker Solar Probe measurements. *The Astrophysical Journal Letters*, *893*(2), 93. https://doi.org/10.3847/1538-4357/ab7f2d

Krieger, A. S., Timothy, A. F., & Roelof, E. C. (1973). A coronal hole and its identification as the source of a high velocity solar wind stream. *Solar Physics*, *29*(2), 505–525. https://doi.org/10.1007/BF00150828

Landi, S., Hellinger, P., & Velli, M. (2006). Heliospheric magnetic field polarity inversions driven by radial velocity field structures. *Geophysical Research Letters*, *33*(14), L14101. https://doi.org/10.1029/2006GL026308

Levine, R. H., Altschuler, M. D., & Harvey, J. W. (1977). Solar sources of the interplanetary magnetic field and solar wind. *Journal of Geophysical Research*, *82*(7), 1061. https://doi.org/10.1029/JA082i007p01061

Lopez, R. E., & Freeman, J. W. (1986). Solar wind proton temperature-velocity relationship. *Journal of Geophysical Research*, *91*(A2), 1701–1705. https://doi.org/10.1029/JA091iA02p01701

Marsch, E., Ao, X. Z., & Tu, C. Y. (2004). On the temperature anisotropy of the core part of the proton velocity distribution function in the solar wind. *Journal of Geophysical Research*, *109*(A4), A04102. https://doi.org/10.1029/2003JA010330

Marsch, E., Mühlhäuser, K.-H., Rosenbauer, H., Schwenn, R., & Denskat, K. U. (1981). Pronounced proton core temperature anisotropy, ion differential speed, and simultaneous Alfvén wave activity in slow solar wind at 0.3 AU. *Journal of Geophysical Research*, *86*(A11), 9199–9203. https://doi.org/10.1029/JA086iA11p09199

Marsch, E., Mühlhäuser, K.-H., Rosenbauer, H., Schwenn, R., & Neubauer, F. M. (1982). Solar wind helium ions: Observations of the Helios solar probes between 0.3 and 1 AU. *Journal of Geophysical Research*, *87*(A1), 35–51. https://doi.org/10.1029/JA087iA01p00035

Marsch, E., Mühlhäuser, K.-H., Schwenn, R., Rosenbauer, H., Pilipp, W., & Neubauer, F. M. (1982). Solar wind protons: Three-dimensional velocity distributions and derived plasma parameters measured between 0.3 and 1 AU. *Journal of Geophysical Research*, *87*(A1), 52–72. https://doi.org/10.1029/JA087iA01p00052

Maruca, B. A., Bale, S. D., Sorriso-Valvo, L., Kasper, J. C., & Stevens, M. L. (2013). Collisional thermalization of hydrogen and helium in solar-wind plasma. *Physical Review Letters*, *111*(24), 241101. https://doi.org/10.1103/PhysRevLett.111.241101

Maruca, B. A., Kasper, J. C., & Gary, S. P. (2012). Instability-driven limits on helium temperature anisotropy in the solar wind: Observations and linear Vlasov analysis. *The Astrophysical Journal Letters*, *748*(2), 137. https://doi.org/10.1088/0004-637X/748/2/137

Matteini, L., Hellinger, P., Goldstein, B. E., Landi, S., Velli, M., & Neugebauer, M. (2013). Signatures of kinetic instabilities in the solar wind. *Journal of Geophysical Research: Space Physics*, *118*(6), 2771–2782. https://doi.org/10.1002/jgra.50320

Matteini, L., Horbury, T. S., Neugebauer, M., & Goldstein, B. E. (2014). Dependence of solar wind speed on the local magnetic field orientation: Role of Alfvénic fluctuations. *Geophysical Research Letters*, *41*(2), 259–265. https://doi.org/10.1002/2013GL058482

Matteini, L., Horbury, T. S., Pantellini, F., Velli, M., & Schwartz, S. J. (2015). Ion kinetic energy conservation and magnetic field strength constancy in multi-fluid solar wind Alfvénic turbulence. *The Astrophysical Journal Letters*, *802*(1), 11. https://doi.org/10.1088/0004-637X/802/1/11

Matteini, L., Stansby, D., Horbury, T. S., & Chen, C. H. K. (2018). On the 1/f spectrum in the solar wind and its connection with magnetic compressibility. *The Astrophysical Journal Letters*, *869*(2), L32. https://doi.org/10.3847/2041-8213/aaf573

Matthaeus, W. H., Elliott, H. A., & McComas, D. J. (2006). Correlation of speed and temperature in the solar wind. *Journal of Geophysical Research*, *111*(A10), A10103. https://doi.org/10.1029/2006JA011636

McComas, D. J., Goldstein, R., Gosling, J. T., & Skoug, R. M. (2001). Ulysses' second orbit: Remarkably different solar wind. *Space Science Reviews*, *97*, 99–103. https://doi.org/10.1023/A:101182611133010.1007/978-94-017-3230-7_16

McManus, M. D., Bowen, T. A., Mallet, A., Chen, C. H. K., Chandran, B. D. G., Bale, S. D., et al. (2020). Cross helicity reversals in magnetic switchbacks. *The Astrophysical Journal Supplement Series*, *246*(2), 67. https://doi.org/10.3847/1538-4365/ab6dce

Mozer, F. S., Agapitov, O. V., Bale, S. D., Bonnell, J. W., Case, T., Chaston, C. C., et al. (2020). Switchbacks in the solar magnetic field: Their evolution, their content, and their effects on the plasma. *The Astrophysical Journal Supplement Series*, *246*(2), 68. https://doi.org/10.3847/1538-4365/ab7196

Neugebauer, M., Forsyth, R. J., Galvin, A. B., Harvey, K. L., Hoeksema, J. T., Lazarus, A. J., et al. (1998). Spatial structure of the solar wind and comparisons with solar data and models. *Journal of Geophysical Research*, *103*(A7), 14587–14599. https://doi.org/10.1029/98JA00798

Neugebauer, M., Goldstein, B. E., Smith, E. J., & Feldman, W. C. (1996). Ulysses observations of differential alpha-proton streaming in the solar wind. *Journal of Geophysical Research*, *101*(A8), 17047–17055. https://doi.org/10.1029/96JA01406

Osman, K. T., Matthaeus, W. H., Greco, A., & Servidio, S. (2011). Evidence for inhomogeneous heating in the solar wind. *The Astrophysical Journal Letters*, *727*(1), L11. https://doi.org/10.1088/2041-8205/727/1/L11

Osman, K. T., Matthaeus, W. H., Hnat, B., & Chapman, S. C. (2012). Kinetic signatures and intermittent turbulence in the solar wind plasma. *Physical Review Letters*, *108*(26), 261103. https://doi.org/10.1103/PhysRevLett.108.261103

Panasenco, O., Velli, M., D'Amicis, R., Shi, C., Réville, V., Bale, S. D., et al. (2020). Exploring solar wind origins and connecting plasma flows from the Parker Solar Probe to 1 AU: Nonspherical source surface and Alfvénic fluctuations. *The Astrophysical Journal Supplement Series*, *246*(2), 54. https://doi.org/10.3847/1538-4365/ab61f4

Panasenco, O., Velli, M., & Panasenco, A. (2019). Large-scale magnetic funnels in the solar corona. *The Astrophysical Journal Letters*, *873*(1), 25. https://doi.org/10.3847/1538-4357/ab017c

Parashar, T. N., Goldstein, M. L., Maruca, B. A., Matthaeus, W. H., Ruffolo, D., Bandyopadhyay, R., et al. (2020). Measures of scale-dependent Alfvénicity in the first PSP solar encounter. *The Astrophysical Journal Supplement Series*, *246*(2), 58. https://doi.org/10.3847/1538-4365/ab64e6

Perrone, D., Alexandrova, O., Roberts, O. W., Lion, S., Lacombe, C., Walsh, A., et al. (2017). Coherent structures at ion scales in fast solar wind: Cluster observations. *The Astrophysical Journal Letters*, *849*(1), 49. https://doi.org/10.3847/1538-4357/aa9022

Perrone, D., Bruno, R., D'Amicis, R., Telloni, D., De Marco, R., Stangalini, M., et al. (2020). Coherent events at ion scales in the inner heliosphere: Parker solar probe observations during the first Encounter. *The Astrophysical Journal*. *905*(2), 142. https://doi.org/10.3847/1538-4357/abc480

Perrone, D., D'Amicis, R., De Marco, R., Matteini, L., Stansby, D., Bruno, R., & Horbury, T. S. (2020). Highly Alfvénic slow solar wind at 0.3 au during a solar minimum: Helios insights for Parker Solar Probe and solar orbiter. *Astronomy & Astrophysics*, *633*, A166. https://doi.org/10.1051/0004-6361/201937064

Perrone, D., Stansby, D., Horbury, T. S., & Matteini, L. (2019). Thermodynamics of pure fast solar wind: radial evolution of the temperature-speed relationship in the inner heliosphere. *Monthly Notices of the Royal Astronomical Society*, *488*(2), 2380–2386. https://doi.org/10.1093/mnras/stz1877

Perrone, D., Valentini, F., Servidio, S., Dalena, S., & Veltri, P. (2014). Analysis of intermittent heating in a multi-component turbulent plasma. *The European Physical Journal*, *68*(7), 209. https://doi.org/10.1140/epjd/e2014-50152-1

Platten, S. J., Parnell, C. E., Haynes, A. L., Priest, E. R., & Mackay, D. H. (2014). The solar cycle variation of topological structures in the global solar corona. *Astronomy & Astrophysics*, *565*, A44. https://doi.org/10.1051/0004-6361/201323048

Podesta, J. J., Roberts, D. A., & Goldstein, M. L. (2006). Power spectrum of small-scale turbulent velocity fluctuations in the solar wind. *Journal of Geophysical Research*, *111*(A10), A10109. https://doi.org/10.1029/2006JA011834

Podesta, J. J., Roberts, D. A., & Goldstein, M. L. (2007). Spectral exponents of kinetic and magnetic energy spectra in solar wind turbulence. *The Astrophysical Journal Letters*, *664*(1), 543–548. https://doi.org/10.1086/519211

Qudsi, R. A., Maruca, B. A., Matthaeus, W. H., Parashar, T. N., Bandyopadhyay, R., Chhiber, R., et al. (2020). Observations of heating along intermittent structures in the inner heliosphere from PSP data. *The Astrophysical Journal Supplement Series*, *246*(2), 46. https://doi.org/10.3847/1538-4365/ab5c19

Réville, V., Velli, M., Panasenco, O., Tenerani, A., Shi, C., Badman, S. T., et al. (2020). The role of Alfvén wave dynamics on the large-scale properties of the solar wind: Comparing an MHD simulation with Parker Solar Probe E1 data. *The Astrophysical Journal Supplement Series*, *246*(2), 24. https://doi.org/10.3847/1538-4365/ab4fef

Riley, P., Downs, C., Linker, J. A., Mikic, Z., Lionello, R., & Caplan, R. M. (2019). Predicting the structure of the solar corona and inner heliosphere during Parker Solar Probe's first perihelion pass. *The Astrophysical Journal Letters*, *874*(2), L15. https://doi.org/10.3847/2041-8213/ab0ec3

Roberts, D. A. (2010). Evolution of the spectrum of solar wind velocity fluctuations from 0.3 to 5 AU. *Journal of Geophysical Research*, *115*(A12). https://doi.org/10.1029/2009JA015120

Salem, C., Mangeney, A., Bale, S. D., & Veltri, P. (2009). Solar wind magnetohydrodynamics turbulence: Anomalous scaling and role of intermittency. *The Astrophysical Journal Letters*, *702*(1), 537–553. https://doi.org/10.1088/0004-637X/702/1/537

Schwartz, S. J., & Marsch, E. (1983). The radial evolution of a single solar wind plasma parcel. *Journal of Geophysical Research*, *88*(A12), 9919–9932. https://doi.org/10.1029/JA088iA12p09919

Schwenn, R. (2006). Solar wind sources and their variations over the solar cycle. *Space Science Reviews*, *124*(1–4), 51–76. https://doi.org/10.1007/s11214-006-9099-5

Smith, E. J., Tsurutani, B. T., & Rosenberg, R. L. (1978). Observations of the interplanetary sector structure up to heliographic latitudes of 16°: Pioneer 11. *Journal of Geophysical Research*, *83*(A2), 717–724. https://doi.org/10.1029/JA083iA02p00717

Stakhiv, M., Landi, E., Lepri, S. T., Oran, R., & Zurbuchen, T. H. (2015). On the origin of mid-latitude fast wind: Challenging the two-state solar wind paradigm. *The Astrophysical Journal Letters 801*(2), 100. https://doi.org/10.1088/0004-637X/801/2/100

Stansby, D., Horbury, T. S., & Matteini, L. (2018). Diagnosing solar wind origins using in situ measurements in the inner heliosphere. *Monthly Notices of the Royal Astronomical Society*, *482*(2), 1706–1714. https://doi.org/10.1093/mnras/sty2814

Stansby, D., Matteini, L., Horbury, T. S., Perrone, D., D'Amicis, R., & Berčič, L. (2020). The origin of slow Alfvénic solar wind at solar minimum. *Monthly Notices of the Royal Astronomical Society*, *492*(1), 39–44. https://doi.org/10.1093/mnras/stz3422

Stansby, D., Perrone, D., Matteini, L., Horbury, T. S., & Salem, C. S. (2019). Alpha particle thermodynamics in the inner heliosphere fast solar wind. *Astronomy & Astrophysics*, *623*, L2. https://doi.org/10.1051/0004-6361/201834900

Telloni, D., & Bruno, R. (2016). Linking fluid and kinetic scales in solar wind turbulence. *Monthly Notices of the Royal Astronomical Society: Letters*, *463*(1), L79–L83. https://doi.org/10.1093/mnrasl/slw135

Telloni, D., Bruno, R., D'Amicis, R., Carbone, F., Marco, R. D., & Perrone, D. (2020). Wave-polarization analysis of the Alfvénic slow solar wind at kinetic scales. *The Astrophysical Journal Letters*, *897*(2), 167. https://doi.org/10.3847/1538-4357/ab980a

Telloni, D., Bruno, R., & Trenchi, L. (2015). Radial evolution of spectral characteristics of magnetic field fluctuations at proton scales. *The Astrophysical Journal Letters*, *805*(1), 46. https://doi.org/10.1088/0004-637X/805/1/46

Tsurutani, B. T., Ho, C. M., Smith, E. J., Neugebauer, M., Goldstein, B. E., Mok, J. S., et al. (1994). The relationship between interplanetary discontinuities and Alfvén waves: Ulysses observations. *Geophysical Research Letters*, *21*(21), 2267–2270. https://doi.org/10.1029/94GL02194

von Steiger, R. (2008). The solar wind throughout the solar cycle. In A. Balogh, L. J. Lanzerotti, & S. T. Suess (Eds.), *The heliosphere through the solar activity cycle* (p. 41). https://doi.org/10.1007/978-3-540-74302-6_3

von Steiger, R., Geiss, J., & Gloeckler, G. (1997). Composition of the Solar Wind. In J. R. Jokipii, C. P. Sonett, & M. S. Giampapa (Eds.), *Cosmic winds and the heliosphere* (p. 581). Tucson: Univ. of Arizona Press.

von Steiger, R., Schwadron, N. A., Fisk, L. A., Geiss, J., Gloeckler, G., Hefti, S., et al. (2000). Composition of quasi-stationary solar wind flows from Ulysses/Solar wind ion composition spectrometer. *Journal of Geophysical Research*, *105*(A12), 27217–27238. https://doi.org/10.1029/1999JA000358

Wang, X., Tu, C., He, J., & Wang, L. (2018). On the full-range β dependence of ion-scale spectral break in the solar wind turbulence. *The Astrophysical Journal Letters*, *857*(2), 136. https://doi.org/10.3847/1538-4357/aab960

Wang, X., Tu, C. Y., He, J. S., & Wang, L. H. (2018). Ion-scale spectral break in the normal plasma beta range in the solar wind turbulence. *Journal of Geophysical Research: Space Physics*, *123*(1), 68–75. https://doi.org/10.1002/2017JA024813

Wang, Y.-M. (1994). Two types of slow solar wind. *The Astrophysical Journal Letters*, *437*, L67. https://doi.org/10.1086/187684

Wang, Y.-M., & Ko, Y.-K. (2019). Observations of slow solar wind from equatorial coronal holes. *The Astrophysical Journal Letters*, *880*(2), 146. https://doi.org/10.3847/1538-4357/ab2add

Wang, Y.-M., & Panasenco, O. (2019). Observations of solar wind from earth-directed coronal pseudostreamers. *The Astrophysical Journal Letters*, *872*(2), 139. https://doi.org/10.3847/1538-4357/aaff5e

Wang, Y.-M., & Sheeley, N. R. Jr. (1990a). Magnetic flux transport and the sunspot-cycle evolution of coronal holes and their wind streams. *The Astrophysical Journal Letters*, *365*, 372. https://doi.org/10.1086/169492

Wang, Y.-M., & Sheeley, N. R. Jr (1990b). Solar wind speed and coronal flux-tube expansion. *The Astrophysical Journal Letters*, *355*, 726. https://doi.org/10.1086/168805

Woodham, L. D., Wicks, R. T., Verscharen, D., & Owen, C. J. (2018). The role of proton cyclotron resonance as a dissipation mechanism in solar wind turbulence: A statistical study at ion-kinetic scales. *The Astrophysical Journal Letters*, *856*(1), 49. https://doi.org/10.3847/1538-4357/aab03d

Wu, P., Perri, S., Osman, K., Wan, M., Matthaeus, W. H., Shay, M. A., et al. (2013). Intermittent heating in solar wind and kinetic simulations. *The Astrophysical Journal Letters*, *763*(2), L30. https://doi.org/10.1088/2041-8205/763/2/L30

Xu, F., & Borovsky, J. E. (2015). A new four-plasma categorization scheme for the solar wind. *Journal of Geophysical Research: Space Physics*, *120*(1), 70–100. https://doi.org/10.1002/2014JA020412

Yamauchi, Y., Suess, S. T., & Sakurai, T. (2002). Relation between pressure balance structures and polar plumes from Ulysses high latitude observations. *Geophysical Research Letters*, *29*(10), 21. https://doi.org/10.1029/2001GL013820

Zank, G. P., Adhikari, L., Hunana, P., Shiota, D., Bruno, R., & Telloni, D. (2017). Theory and transport of nearly incompressible magnetohydrodynamic turbulence. *The Astrophysical Journal Letters*, *835*(2), 147. https://doi.org/10.3847/1538-4357/835/2/147

Zank, G. P., & Matthaeus, W. H. (1992). Waves and turbulence in the solar wind. *Journal of Geophysical Research*, *97*(A11), 17189–17194. https://doi.org/10.1029/92JA01734

Zhao, L., Zurbuchen, T. H., & Fisk, L. A. (2009). Global distribution of the solar wind during solar cycle 23: ACE observations. *Geophysical Research Letters*, *36*(14), L14104. https://doi.org/10.1029/2009GL039181

Zirker, J. B. (1977). Coronal holes and high-speed wind streams. *Review of Geophysics*, *15*, 257–269. https://doi.org/10.1029/RG015i003p00257

Zurbuchen, T. H. (2007). A new view of the coupling of the sun and the heliosphere. *Annual Review of Astronomy and Astrophysics*, *45*(1), 297–338. https://doi.org/10.1146/annurev.astro.45.010807.154030

Zurbuchen, T. H., Hefti, S., Fisk, L. A., Gloeckler, G., & Schwadron, N. A. (2000). Magnetic structure of the slow solar wind: Constraints from composition data. *Journal of Geophysical Research*, *105*(A8), 18327–18336. https://doi.org/10.1029/1999JA000427

Zurbuchen, T. H., Hefti, S., Fisk, L. A., Gloeckler, G., & von Steiger, R. (1999). The transition between fast and slow solar wind from composition data. *Space Science Reviews*, *87*, 353–356. https://doi.org/10.1023/A:100512671871410.1007/978-94-015-9167-6_62